



1  
2  
3  
4  
5  
6  
7  
8  
9  
10  
11  
12  
13  
14  
15  
16  
17  
18

**A Stratospheric Connection to Atlantic Climate Variability**

Thomas Reichler<sup>1\*</sup>, Junsu Kim<sup>1</sup>, Elisa Manzini<sup>2</sup>, and Jürgen Kröger<sup>2</sup>

<sup>1</sup>Department of Atmospheric Sciences, University of Utah, Salt Lake City, Utah, USA

<sup>2</sup>Max Planck Institute for Meteorology, Hamburg, Germany

Correspondence: Thomas Reichler, [thomas.reichler@utah.edu](mailto:thomas.reichler@utah.edu), 801-585-0040



19 **It is well recognized that the stratosphere is connected to tropospheric weather and**  
20 **climate. In particular, extreme stratospheric circulation events and their dynamical**  
21 **feedback on the troposphere are known to play a major role<sup>1</sup>. However, what is not**  
22 **known to date is whether the state of the stratosphere also matters for the ocean and**  
23 **its circulation. Previous research suggests co-variability of decadal stratospheric**  
24 **flow variations and conditions in the North Atlantic Ocean, but such findings are**  
25 **based on short simulations with only one climate model<sup>2</sup>. Here we report that over**  
26 **the past 30 years the stratosphere and the Atlantic thermohaline circulation**  
27 **underwent low-frequency variations that were similar to each other. Using climate**  
28 **models we demonstrate that this similarity is consistent with the hypothesis that**  
29 **variations in the sequence of stratospheric circulation anomalies, combined with the**  
30 **persistence of individual anomalies, lead to a significant impact of the stratosphere**  
31 **on the North Atlantic Ocean. Our work identifies a previously unknown source for**  
32 **decadal climate variability and suggests that simulations of deep layers of the**  
33 **atmosphere and the ocean are needed for realistic predictions of climate.**

34  
35 The ocean has a large thermal inertia and is dominated by variability on time scales of  
36 years to decades. Traditionally, atmospheric influences on the ocean are understood from  
37 the stochastic climate model paradigm, in which the troposphere is thought to provide a  
38 white-noise forcing that is integrated by the ocean to yield a low-frequency response<sup>3</sup>. In  
39 this study we propose another relevant influence, which is related to the stratosphere. The  
40 stratosphere is characterized by persistent flow dynamics<sup>4</sup> and considerable multi-decadal  
41 energy<sup>5-7</sup>. Variations in the strength of the wintertime northern hemispheric stratospheric

42 vortex, so called “polar vortex events”, are known to last for many weeks, as does their  
 43 impact on the troposphere<sup>8</sup>. An example are stratospheric sudden warmings (SSWs),  
 44 prolonged time periods with an unusually weak and warm polar vortex. SSWs occur on  
 45 average every second year, but observations over the past 30 years reveal an intriguing  
 46 quasi-decadal rhythm in the year-to-year occurrence of such events: during the 1990s, the  
 47 Arctic winter stratosphere was characterized by an almost complete absence of SSWs,  
 48 but during the 1980s and also during the 2000s the stratosphere experienced a record  
 49 number of such events (Fig. 1a).

50 A connection between the stratosphere and the ocean can be established by the  
 51 North Atlantic Oscillation (NAO), a large-scale pattern of near-surface circulation  
 52 anomalies over the North Atlantic. Polar vortex events modulate the NAO polarity, with  
 53 a strong vortex leading to a positive and a weak vortex to a negative NAO<sup>8</sup>. NAO  
 54 variations in turn are linked to circulation variability in the North Atlantic. The NAO  
 55 induces anomalous fluxes of heat, momentum, and freshwater at the air-sea interface,  
 56 driving or perhaps enhancing intrinsic variability in the North Atlantic gyre system<sup>9</sup> and  
 57 the Atlantic Meridional Overturning Circulation (AMOC)<sup>10,11</sup>. Thus, variations in the  
 58 strength of the polar vortex and their projection on the NAO might influence the North  
 59 Atlantic circulation. This is supported by a reconstruction of past AMOC variations using  
 60 twelve different ocean reanalyses, revealing a similarity between variations in the AMOC  
 61 (Fig. 1b) and the frequency of SSWs (Fig. 1a).

62 The observational record is too short for a rigorous analysis of multi-decadal  
 63 variability. Therefore, we examine the climate model GFDL-CM2.1 that was integrated  
 64 for 4000 years with constant forcings, approximately representative for pre-industrial

65 conditions<sup>12</sup>. A connection between stratosphere and ocean depends on the downward  
 66 coupling into the troposphere. We examine this coupling by comparing the simulation  
 67 against atmospheric reanalysis (hereafter simply observations). Focusing on periods  
 68 where the polar vortex is unusually strong, we define events during which the Northern  
 69 Annular Mode index (NAM) at 10 hPa crosses a threshold of 2.5. Our outcomes are not  
 70 very sensitive to the exact threshold, but our choice limits the number of events and  
 71 captures sufficiently strong events. In the observations, we find 22 events, which is an  
 72 average of 4 per decade. At 3.8 per decade, the model produces similar statistics. We  
 73 form composites of observed and simulated events in terms of anomalies in the NAM at  
 74 pressure levels between 1000 and 10 hPa and for various lags. The model captures well  
 75 the structure of downward propagating stratospheric NAM anomalies seen in the  
 76 observations (Fig. 2a and 2b). However, the NAM is normalized and thus not an absolute  
 77 measure of circulation anomaly. This is important because the model does not have a  
 78 well-resolved stratosphere, and, compared to the observations, it underestimates the day-  
 79 to-day variability of zonal mean zonal winds in the stratosphere by about 40%. A more  
 80 objective response measure is the zonal wind stress ( $\tau$ ) over our North Atlantic study  
 81 region (15°W-60°W, 45°N-65°N). For the selected events, the simulated  $\tau$  anomalies are  
 82 considerably smaller than in the observations (Fig. 2c and 2d), which is probably a  
 83 consequence of the inadequate treatment of the model's stratosphere. However, it is  
 84 reassuring that the model reproduces the observed sign and temporal structure of  $\tau$ .

85         The surface impacts of the events examined in Fig. 2 include a north-south dipole  
 86 in sea level pressure, which is a positive phase of the NAO (Fig. 3). The nodal point of  
 87 this dipole is located to the south of Greenland. There, the changes in wind stress amplify

88 the climatological mean westerlies and heat fluxes that extract thermal energy from the  
 89 ocean. The model produces a heat flux pattern (Fig 3. shading) that is very similar to the  
 90 observations, but the sea surface temperature (SST) cooling over the study region is three  
 91 times smaller (Fig. 2c and 2d). This muted SST response is related to the weak wind  
 92 stress forcing, but also to the model's heat distribution in a 10 meter thick top ocean  
 93 layer. The cooling to the south of Greenland is dynamically relevant because it is  
 94 colocated with sites of significant deepwater formation in the Labrador and Irminger Seas  
 95 and with the model's subpolar gyre (SPG) (Supplementary Fig. 2).

96 We now study the ocean response in GFDL-CM2.1 to the stratospherically  
 97 induced cooling. Because low-frequency forcing should be most effective in driving the  
 98 ocean<sup>3</sup>, we composite on a low-pass filtered stratospheric NAM (see methods) using a  
 99 threshold of plus or minus one. From the 4000 years, we identify 75 strong and 70 weak  
 100 events. Results from weak events are multiplied by minus one and combined with the  
 101 strong events to form a single composite. The vortex index (Fig. 4a), which reflects the  
 102 likelihood for a vortex event to occur, shows the outcome of the compositing in terms of  
 103 stratospheric circulation anomalies: the compositing favors strong polar vortex events  
 104 that happen for several consecutive years centered on year zero. This situation is  
 105 comparable to the one seen in the observations over the past 30 years (Fig. 1a).

106 Over our study region, the vortex events induce a  $\sim 0.1^{\circ}\text{K}$  cooling at the ocean  
 107 surface (Fig. 4b). Over the course of a few years, this signal penetrates into the deep  
 108 ocean. The speed and depth of the penetration suggest that deep convection, which  
 109 prevails over this region, is responsible. The cooling is followed by regular oscillations,  
 110 which have a similar periodicity as the model's AMOC (Supplementary Fig. 1). This

111 suggests that the oscillations are connected to the AMOC, which is confirmed when  
 112 compositing the AMOC on the stratospheric events (Fig. 4c). Following the central date,  
 113 the AMOC undergoes regular fluctuations that are coherent with the ocean temperatures.

114       The standard deviation of the low-pass filtered AMOC fluctuations following the  
 115 central date amounts to  $\sim 0.23$  Sv (Fig. 4c). However, for certain strong events this value  
 116 exceeds  $\sim 0.5$  Sv (Supplementary Fig. 3), which can be compared to the  $\sim 1.3$  Sv of the  
 117 model's total AMOC standard deviation. In other words, forcing from the stratosphere  
 118 contributes to a large portion of total AMOC variability. The vigorous intrinsic tendency  
 119 of the model's AMOC to oscillate suggests that the stratosphere acts as trigger for such  
 120 oscillations and that forcing at the resonant frequency is most effective in driving it. This  
 121 is supported by analysis presented in Supplementary Fig. 3.

122       We generalize our results by investigating additional simulations taken from the  
 123 preindustrial control experiment of the Fifth Coupled Model Intercomparison Project  
 124 (CMIP5). For each CMIP5 model, we examine the surface anomalies that develop over  
 125 the study region in response to vortex events (Fig. 5a). As before, strong events are  
 126 associated with increased  $\tau$  and colder SSTs, but there is a large inter-model spread. We  
 127 divide the models into two classes: high-top models with a well-resolved stratosphere,  
 128 and low-top models with a relatively simple stratosphere. The surface response of the  
 129 combined (black) high-top models is significantly stronger than that of the (grey) low-top  
 130 models, confirming our previous assumption about the role of stratospheric  
 131 representation. Using criteria identical to that in Fig. 4, we composite the AMOC time  
 132 series from all high-top (Fig. 5b) and all low-top (Fig. 5c) models on low-frequency  
 133 vortex events. As in GFDL-CM2.1, the AMOC of both multi-model ensembles starts to

134 oscillate after the vortex events. However, while the oscillations persist for decades in  
135 GFDL-CM2.1, they vanish after several years in the CMIP5 ensembles. This is due to the  
136 widely differing spectral characteristics of the AMOC in the models, leading the  
137 composite outcome to de-correlate relatively fast. The magnitude of the AMOC  
138 anomalies after the events reaches ~20% of the climatological standard deviation. It is  
139 about the same for the two model classes, despite the differences in forcing strength at the  
140 surface. This similarity might be related to model differences that go beyond our simple  
141 high-top/low-top classification and the complicated response of the AMOC that involves  
142 non-linear dynamics.

143 Our analysis suggests a significant stratospheric impact on the ocean. Recurring  
144 stratospheric vortex events create long-lived perturbations at the ocean surface, which  
145 penetrate into the deeper ocean and trigger multi-decadal variability in its circulation.  
146 This leads to the remarkable fact that signals that emanate from the stratosphere cross the  
147 entire atmosphere-ocean system. The propagation into the deeper ocean can be explained  
148 from the well-known impact of the NAO on the SPG and AMOC<sup>13,14</sup>. The oscillatory  
149 behavior of the ocean following stratospheric events is likely related to a delayed  
150 negative feedback of the AMOC on itself<sup>11,14,15</sup>. A number of factors promote the  
151 stratosphere-ocean connection: the persistence of individual stratospheric events; a  
152 stratospheric rhythm that matches the resonant frequency of the AMOC; the dynamical  
153 coupling from the stratosphere to the troposphere; the collocation between the NAO  
154 nodal point and regions of downwelling; and the intrinsic instability of the AMOC.

155 We do not advocate the stratosphere as the sole or primary source of AMOC  
156 variability. However, the stratosphere appears to contain a significant amount of low-

157 frequency energy capable of modulating the AMOC. The source of this energy may be  
158 related to coupling with other subcomponents of climate<sup>16-18</sup> or variations in external  
159 forcings<sup>19,20</sup>. However, in our simulations external forcings are held constant in time, and  
160 our analysis (Fig. 4, Supplementary Figs. 4 and 5) leads to the conclusion that at low  
161 frequencies the stratosphere drives the AMOC. It appears most likely to us that the  
162 stratospheric multi-decadal energy is related to stochastic forcing from the  
163 troposphere<sup>21,22</sup>, which may involve variations in the dynamical wave forcing<sup>7</sup>, or in the  
164 frequency of blockings<sup>23</sup> and their influence on SSWs<sup>24</sup>.

165 Our results have implications for the prediction of decadal climate, an area that  
166 has gained increasing attention recently<sup>25-27</sup>. Since it is impossible to accurately predict  
167 variations in the strength of the polar vortex beyond several days, it is likely that the new  
168 mechanism acts to limit the skill of decadal predictions. However, representing the  
169 coupling between stratosphere, troposphere, and ocean in modelling systems should  
170 refine estimates of decadal climate predictability and improve the skill of short-term  
171 climate predictions after strong stratospheric events. Our results add to an increasing  
172 body of evidence that the stratosphere forms an important component of climate and that  
173 this component should be represented well in models.

174  
175



176 **Methods**

177

 178 **Data**

 179 **Observations.** NCEP/NCAR reanalysis (1958-2011) are used as observations of

180 geopotential height, surface fluxes, and SSTs.

 181 **GFDL-CM2.1.** The main model of this study is the Geophysical Fluid Dynamics

182 Laboratory climate model GFDL-CM2.1. It has a horizontal resolution of 2° latitude by

183 2.5° longitude, and 24 vertical levels concentrated in the troposphere, leading to a

184 relatively poorly resolved stratosphere. The model produces realistic simulations of

 185 tropospheric climate<sup>28</sup> and self-sustained AMOC oscillations with a central period of ~20

186 years (Supplementary Fig. 1). Such oscillations may be connected to the Atlantic Multi-

 187 decadal Oscillation (AMO)<sup>29</sup>, a pattern of North Atlantic SST variations with a period of

 188 60-80 years<sup>30</sup>. The fact that the period of the observed AMO is longer than the period of

189 the simulated AMOC is not surprising given the many simplifying physics in climate

190 models and the uncertainty in observing the AMO.

 191 **CMIP5.** CMIP5 data are based on monthly means from the preindustrial control

192 experiment. We consider models that provide at least 500 years of data and the quantities

193 needed for our analysis. This leads to 18 models with a total of 12,944 years of

194 simulation data (Fig. 5a and Supplementary Table 2). In Fig. 5b we perform analysis on

195 the concatenated NAM and AMOC time series from models belonging to either the high-

196 top or the low-top group; time series from each model are standardized before

197 concatenation.

198

 199 **Statistics**

200 **Statistical analysis.** In all our analysis we take the same non-parametric approach to  
 201 establish statistical significance at the two-sided 95% level. In this approach, we  
 202 randomly sub-sample elements from the entire population and take averages. The number  
 203 of elements selected equals the number included in the quantity to be tested. We repeat  
 204 this procedure 10,000 times, leading to a distribution of outcomes that is the result of  
 205 pure chance. The upper and lower 2.5 percentiles of this distribution are our empirically  
 206 determined confidence limits.

207 **Event selection.** The events selected for the composites shown in Fig. 4 and 5b are based  
 208 on the dates on which the smoothed annual November-March means of the NAM at 10  
 209 hPa (Gaussian filter,  $\sigma \sim 2$  years) exceed a value of plus or minus one; selected events are  
 210 separated by at least 30 years.

211 **Detrending.** In order to account for long-term trends we first remove from all quantities  
 212 a low-pass filtered (101-year running means) version of the data. Daily atmospheric  
 213 quantities are filtered by removing a slowly varying trend climatology, following a  
 214 procedure that accounts for seasonality of trends<sup>31</sup>, except that a running mean filter of  
 215 101 years is applied.

216

### 217 **Climate indices**

218 **SSWs.** SSWs are defined when the daily zonal mean zonal wind at 10 hPa becomes  
 219 easterly. Only the first SSW in a given winter is chosen; final warmings are excluded.

220 **SSW index.** The binary SSW index is defined by assigning years with (without) a SSW a  
 221 value of minus (plus) one.



222 **Vortex index.** The model derived “Vortex index” is similar to the “SSW index”; both  
223 measure whether a polar vortex event occurs. Introducing the Vortex index is necessary  
224 because most low-top models have positive stratospheric wind biases, causing wind  
225 reversals and SSWs to become rare. The Vortex index is based on the daily normalized  
226 NAM at 10 hPa and a threshold of plus two (minus three) to identify strong (weak) vortex  
227 years. The index is assigned a value of plus (minus) one if a strong (weak) vortex is  
228 detected; other years (neutral) are assigned a value of zero.

229 **NAM.** The NAM is based on empirical orthogonal function (EOF) analysis performed  
230 individually at each level using daily zonal mean geopotential heights poleward of 20°N;  
231 the NAM is the standardized EOF time series at any level.

232 **NAO.** The NAO is the leading EOF time series of daily sea level pressure over 20°N-  
233 80°N and 90°W-40°E.

234 **AMOC.** The AMOC is the maximum of the North Atlantic meridional overturning  
235 streamfunction at 45°N. For some models, the streamfunction is available as a pre-  
236 calculated CMIP5 quantity. For other models and for the reanalyses, the streamfunction is  
237 derived by vertically integrating the meridional sea water velocity. The reanalysis derived  
238 AMOC (1979-2010) stems from the mean over 12 products (Supplementary Table 1).

239 Prior to taking the multi-reanalysis mean, time series from each reanalysis are  
240 normalized, annually averaged, and smoothed (Gaussian filter,  $\sigma \sim 1.3$  years). All 12  
241 reanalysis are only available for the 1993-2001 period. Outside this period, fewer  
242 reanalyses exist, creating spurious discontinuities at the interface between the full and the  
243 reduced set. We adjust for this by removing from the reduced set the difference between  
244 the full and reduced set at the interface.



245 **AMO.** The AMO is the monthly mean SST average over 0°N-60°N and 75°W-7.5°W<sup>19</sup>.

246

247 **References**

248

249 1 Baldwin, M. P., Thompson, D. W. J., Shuckburgh, E. F., Norton, W. A. &amp; Gillett,

250 N. P. Weather from the Stratosphere? *Science* **301**, 317-319 (2003).

251 2 Manzini, E., Cagnazzo, C., Fogli, P. G., Bellucci, A. &amp; Müller, W. A.

252 Stratosphere-troposphere coupling at inter-decadal time scales: Implications for

253 the North Atlantic Ocean. *Geophys. Res. Lett.* **39**, L05801 (2012).254 3 Hasselmann, K. Stochastic climate models Part I. Theory. *Tellus* **28**, 473-485

255 (1976).

256 4 Baldwin, M. P. *et al.* Stratospheric memory and extended-range weather257 forecasts. *Science* **301**, 636-640 (2003).

258 5 Cohen, J., Barlow, M. &amp; Saito, K. Decadal Fluctuations in Planetary Wave

259 Forcing Modulate Global Warming in Late Boreal Winter. *J. Climate* **22**, 4418-

260 4426 (2009).

261 6 Gillett, N. P. *et al.* How linear is the Arctic Oscillation response to greenhouse262 gases? *J. Geophys. Res.* **107**, 4022 (2002).

263 7 Butchart, N., Austin, J., Knight, J. R., Scaife, A. A. &amp; Gallani, M. L. The

264 Response of the Stratospheric Climate to Projected Changes in the Concentrations

265 of Well-Mixed Greenhouse Gases from 1992 to 2051. *J. Climate* **13**, 2142-2159

266 (2000).

267 8 Baldwin, M. P. &amp; Dunkerton, T. J. Stratospheric harbingers of anomalous weather

268 regimes. *Science* **294**, 581-584 (2001).

269 9 Hakkinen, S. &amp; Rhines, P. B. Decline of Subpolar North Atlantic Circulation

270 During the 1990s. *Science* **304**, 555-559 (2004).



- 271 10 Delworth, T. L. & Greatbatch, R. J. Multidecadal Thermohaline Circulation  
272 Variability Driven by Atmospheric Surface Flux Forcing. *J. Climate* **13**, 1481-  
273 1495 (2000).
- 274 11 Eden, C. & Jung, T. North Atlantic Interdecadal Variability: Oceanic Response to  
275 the North Atlantic Oscillation (1865-1997). *J. Climate* **14**, 676-691 (2001).
- 276 12 Wittenberg, A. T. Are historical records sufficient to constrain ENSO  
277 simulations? *Geophys. Res. Lett.* **36**, L12702 (2009).
- 278 13 Häkkinen, S. Variability of the simulated meridional heat transport in the North  
279 Atlantic for the period 1951-1993. *J. Geophys. Res.* **104**, 10991-11007 (1999).
- 280 14 Lohmann, K., Drange, H. & Bentsen, M. A possible mechanism for the strong  
281 weakening of the North Atlantic subpolar gyre in the mid-1990s. *Geophys. Res.*  
282 *Lett.* **36**, L15602 (2009).
- 283 15 Delworth, T., Manabe, S. & Stouffer, R. J. Interdecadal Variations of the  
284 Thermohaline Circulation in a Coupled Ocean-Atmosphere Model. *J. Climate* **6**,  
285 1993-2011 (1993).
- 286 16 Msadek, R., Frankignoul, C. & Li, L. Mechanisms of the atmospheric response to  
287 North Atlantic multidecadal variability: a model study. *Clim. Dynam.* **36**, 1255-  
288 1276 (2011).
- 289 17 Mosedale, T. J., Stephenson, D. B., Collins, M. & Mills, T. C. Granger Causality  
290 of Coupled Climate Processes: Ocean Feedback on the North Atlantic Oscillation.  
291 *J. Climate* **19**, 1182-1194 (2006).



- 292 18 Cohen, J., Barlow, M., Kushner, P. J. & Saito, K. Stratosphere-Troposphere  
293 Coupling and Links with Eurasian Land Surface Variability. *J. Climate* **20**, 5335-  
294 5343 (2007).
- 295 19 Ottera, O. H., Bentsen, M., Drange, H. & Suo, L. External forcing as a  
296 metronome for Atlantic multidecadal variability. *Nature Geosci.* **3**, 688-694  
297 (2010).
- 298 20 Ineson, S. *et al.* Solar forcing of winter climate variability in the Northern  
299 Hemisphere. *Nature Geosci.* **4**, 753-757 (2011).
- 300 21 Scaife, A. A., Knight, J. R., Vallis, G. K. & Folland, C. K. A stratospheric  
301 influence on the winter NAO and North Atlantic surface climate. *Geophys. Res.*  
302 *Lett.* **32**, L18715 (2005).
- 303 22 Plumb, R. A. & Semeniuk, K. Downward migration of extratropical zonal wind  
304 anomalies. *J. Geophys. Res.* **108** (D7), 4223, doi:4210.1029/2002JD002773  
305 (2003).
- 306 23 Hakkinen, S., Rhines, P. B. & Worthen, D. L. Atmospheric Blocking and Atlantic  
307 Multidecadal Ocean Variability. *Science* **334**, 655-659 (2011).
- 308 24 Martius, O., Polvani, L. M. & Davies, H. C. Blocking precursors to stratospheric  
309 sudden warming events. *Geophys. Res. Lett.* **36**, L14806 (2009).
- 310 25 Keenlyside, N. S., Latif, M., Jungclaus, J., Kornblueh, L. & Roeckner, E.  
311 Advancing decadal-scale climate prediction in the North Atlantic sector. *Nature*  
312 **453**, 84-88 (2008).
- 313 26 Smith, D. M. *et al.* Skilful multi-year predictions of Atlantic hurricane frequency.  
314 *Nature Geosci.* **3**, 846-849 (2010).

- 315 27 Mehta, V. *et al.* Decadal Climate Predictability and Prediction: Where Are We?  
316 *Bull. Amer. Meteor. Soc.* **92**, 637-640 (2011).
- 317 28 Reichler, T. & Kim, J. How well do coupled models simulate today's climate?  
318 *Bull. Amer. Meteor. Soc.* **89**, 303-311 (2008).
- 319 29 Delworth, T. L. & Mann, M. E. Observed and simulated multidecadal variability  
320 in the Northern Hemisphere. *Clim. Dynam.* **16**, 661-676 (2000).
- 321 30 Schlesinger, M. E. & Ramankutty, N. An oscillation in the global climate system  
322 of period 65-70 years. *Nature* **367**, 723-726 (1994).
- 323 31 Gerber, E. P. *et al.* Stratosphere-troposphere coupling and annular mode  
324 variability in chemistry-climate models. *J. Geophys. Res.* **115**, D00M06 (2010).
- 325
- 326
- 327



328

329 **Corresponding author**

330 Correspondence to: Thomas Reichler

331

332 **Acknowledgements**

333 We thank Tom Delworth, Paul Staten, and Court Strong for their comments on an earlier  
334 version of this work. We thank the Geophysical Fluid Dynamics Laboratory for making  
335 the CM2.1 simulation data available to us. We acknowledge the World Climate Research  
336 Programm's Working Group on Coupled Modeling, which is responsible for CMIP, and  
337 we thank the climate modeling groups for producing and making available their model  
338 output. For CMIP the U.S. Department of Energy's Program for Climate Model  
339 Diagnosis and Intercomparison provides coordinating support and led development of  
340 software infrastructure in partnership with the Global Organization for Earth System  
341 Science Portals. This research used resources of the National Energy Research Scientific  
342 Computing Center, which is supported by the Office of Science of the U.S. Department  
343 of Energy under Contract No. DE-AC02-05CH11231. T.R. and J.K. were supported by  
344 the University of Utah. E.M. and J.K. are grateful for partial funding by the European  
345 Commission's 7<sup>th</sup> Framework Programme, under GA 226520, COMBINE project.  
346 Provision of computer infrastructure by the Center for High Performance Computing at  
347 the University of Utah is gratefully acknowledged.

348

349

350 **Author contributions**

351 T.R. designed the research and wrote the manuscript. J.K. carried out the analysis. All  
352 authors contributed to the interpretations of the results and the discussion of the  
353 manuscript.

354

355 **Competing financial interests**

356

357 The authors declare no competing financial interests.

358

359

360

361 **Figure legends**

362

363 **Figure 1: Observed stratospheric flow variations and their relationship to AMOC.**

364 **a**, Annual time series of the SSW index; grey bars mark years (-1) with and (1) without  
 365 major SSWs, and black line is smoothed version of it. **b**, Multi-reanalysis estimate of  
 366 annual mean AMOC variations at 45°N; thick black line denotes the common period for  
 367 all 12 reanalyses and grey shading is the  $\pm 1\sigma$  uncertainty interval.

368

369 **Figure 2: Strong polar vortex composites and their surface impact. a and b**, Time-

370 height development of NAM index; white contours indicate NAM values of one and two.

371 Horizontal time axis indicates the lead or lag (in days) with respect to the date of the  
 372 events. The events are determined by the dates on which the NAM at 10 hPa crosses plus  
 373 2.5. **c and d**, Associated (red) zonal wind stress and (black) SST anomalies over the  
 374 North Atlantic study region; numbers at the upper right are averages over days 0-60.

375

376 **Figure 3: Spatial pattern of surface impact from the stratosphere.** Shown are

377 composite anomalies averaged from day 0 to 60 following the strong vortex events of  
 378 Fig. 2. Sea level pressure anomalies are contoured at  $\pm 0.5$ ,  $\pm 1$ ,  $\pm 2$ ,  $\pm 3$ ,  $\pm 4$  hPa; red (blue)  
 379 lines indicate positive (negative) values. Shading shows the sum of latent and sensible  
 380 heat flux anomalies (in  $\text{Wm}^{-2}$ ), with positive (negative) anomalies indicating oceanic heat  
 381 gain (loss). Vectors represent magnitude and direction of surface wind stress anomalies.

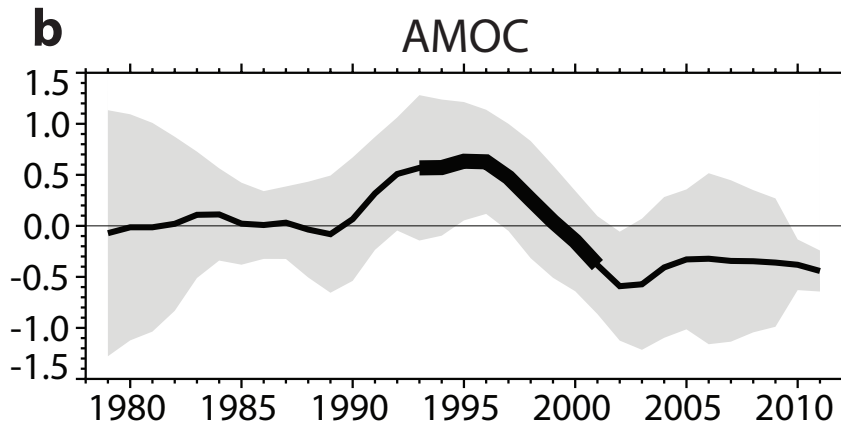
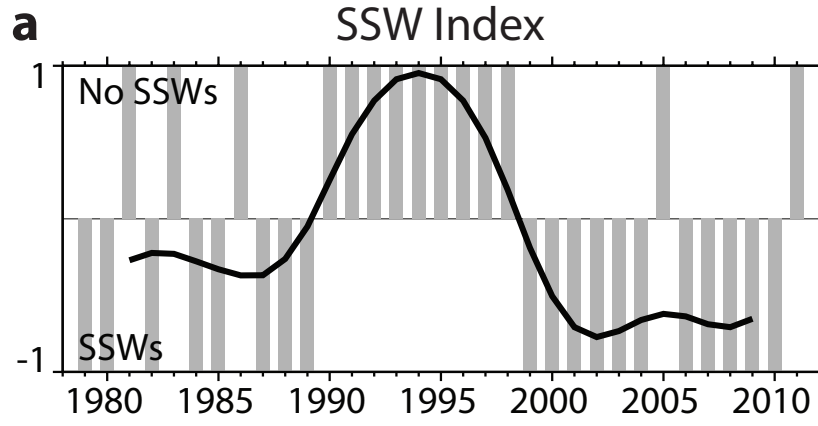
382

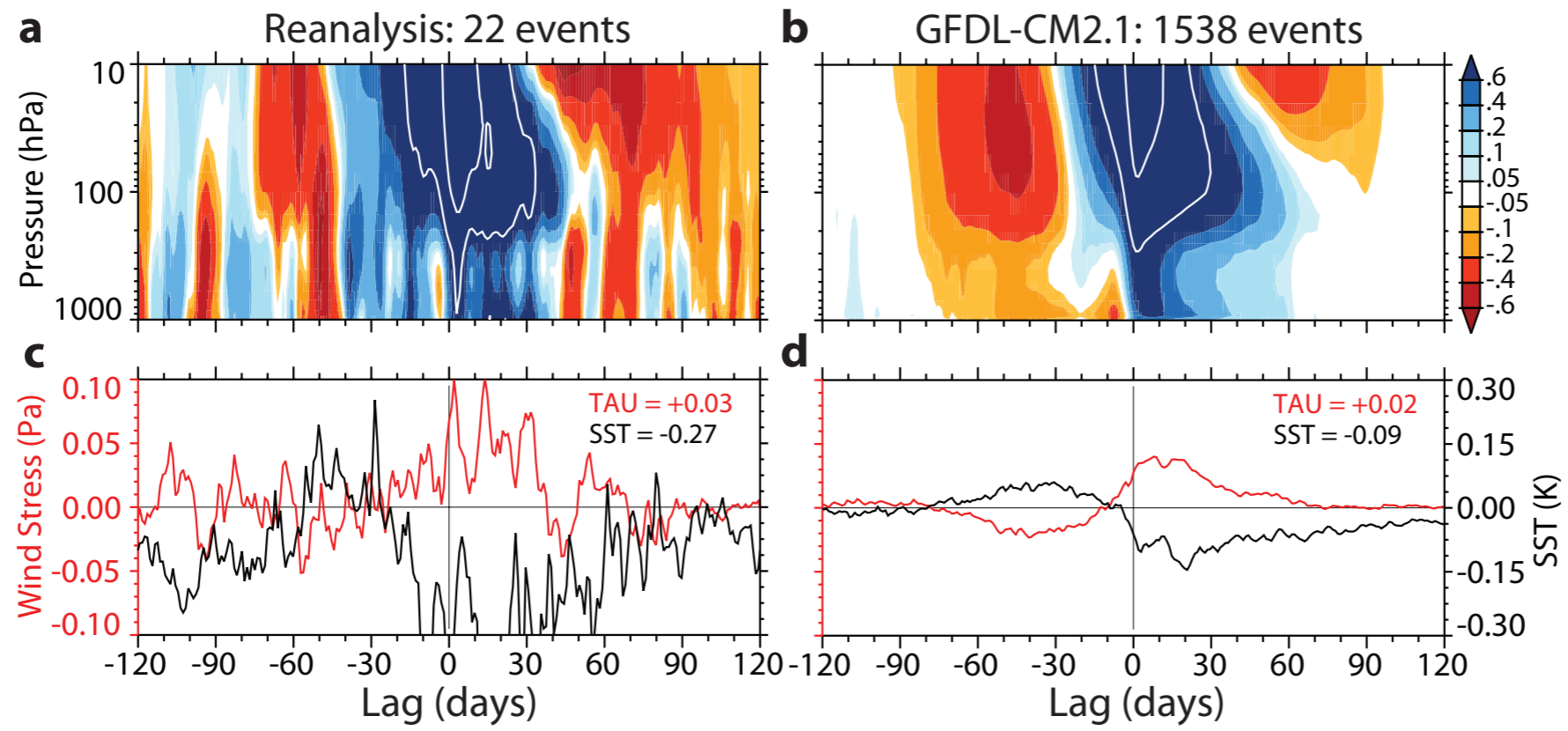
383 **Figure 4: Impact of persistent stratospheric flow variations.** Shown are GFDL-CM2.1

384 derived composites of periods during which the polar vortex was either persistently

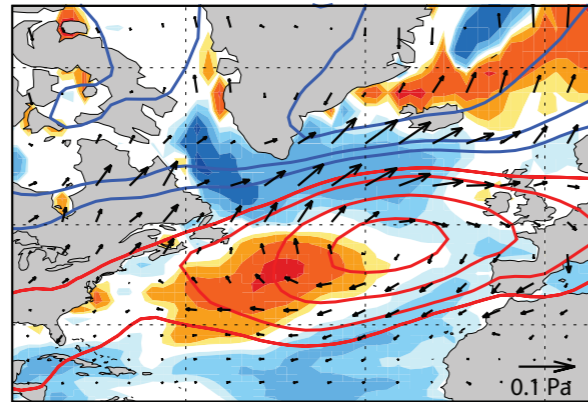
385 strong (75 events) or persistently weak (70 events, multiplied by minus one). **a**,  
 386 Composite time series of the Vortex index, measuring the likelihood that a vortex event  
 387 happens during a given year. The index represents a composite and therefore varies  
 388 smoothly between plus and minus one. **b**, Corresponding monthly time-depth  
 389 development of ocean temperature anomalies (K) over the study region (15°W-60°W,  
 390 45°N-65°N); hatching shows insignificant (95%) results. **c**, Corresponding monthly  
 391 anomalies in AMOC strength (Sv).  
 392

393 **Figure 5: CMIP5 composites on stratospheric NAM.** **a**, Standardized TAU and SST  
 394 anomalies over study region for individual models and mean of all low-top and all high-  
 395 top models; the anomalies are averages over months 1-2 (TAU) and 1-3 (SST) following  
 396 the NAM events. Thresholds of plus 2.5 and minus 3 in monthly NAM define the events.  
 397 Circles are 95% uncertainty intervals (see methods). **b** and **c**, Standardized AMOC  
 398 anomalies from the high-top (low-top) models composited on persistent NAM events; the  
 399 events are defined as in Fig. 4 and contain 127 (143) strong and 133 (144) weak events  
 400 for LOW (HIGH).  
 401





**a** Reanalysis: 22 events



**b** GFDL-CM2.1: 1538 events

